Molecular determinants in the hemagglutinin gene associated with the emergence of highly pathogenic avian influenza H7N9 virus in China

Yue Ji, Wen Su, Ka Tim Choy, Hui-Ling Yen

School of Public Health, Li Ka Shing Faculty of Medicine, The University of Hong Kong, Hong Kong Special Administrative Region, China

INTRODUCTION

Low pathogenic avian influenza viruses (LPAIV) of H5 and H7 subtypes possess the potential to evolve to the highly pathogenic form (HPAIV), by acquiring a multi-basic amino acid motif at the hemagglutinin (HA) cleavage site that expands the HA cleavability by intracellular proteases and viral tissue tropism. The Asian H7N9 LPAIV that cause zoonotic infections in humans since 2013 evolved into HPAIV in 2016, after a four-year-circulation among poultry in China. Polymorphism at HA cleavage site has been identified among H7N9 HPAIV field isolates, with two dominant sequences reported PKGKRTAR/G and PKRKRTAR/G. We showed that the two motifs possess different cleavability in avian and mammal cell lines. The HA gene of the H7N9 LPAIV can be phylogenetically classified into two lineages, Yangtze River Delta (YRD) and Pearl River Delta (PRD) lineages, while the H7N9 HPAIV were only clustered with the YRD-like viruses. We hypothesized that specific molecular determinants in the HA gene of the YRD-like viruses may have assisted the insertion of the multi-basic amino acid motif at the HA cleavage sites.

METHODS

1. Recombinant viruses used for determine the cleavability of the HA protein containing different cleavage sites (Figure 1a).

2. Parental recombinant viruses (Figure 1b) and serial passage in 14-day eggs (Figure 1c).

A

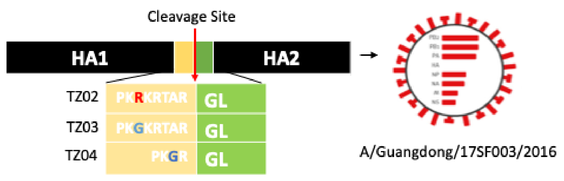

C

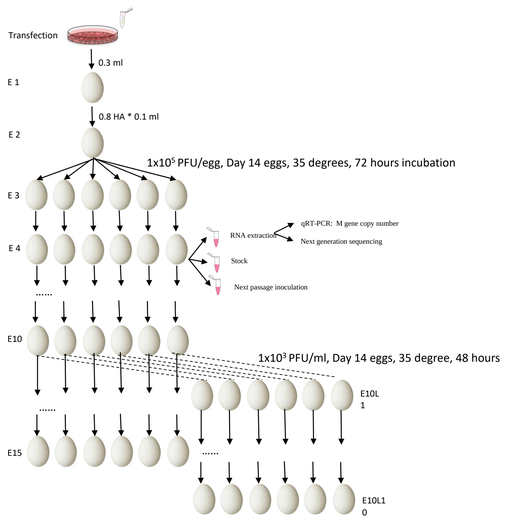

B

Abb.	Virus Name	Segments							
		PB1	PB2	PA	HA	NP	NA	M	NS
YRD	Rg-A/Dressed chicken/GD/GZ631/2017 x YRD-HA								
YRDQ	Rg-A/Dressed chicken/GD/GZ631/2017 x YRD-HA^{L226Q}				L226Q				
PRD	Rg-A/Dressed chicken/GD/GZ631/2017 x PRD-HA								
IYRD	Rg-A/Dressed chicken/GD/GZ631/2017 (PB1^{V43I}) x YRD-HA	V43I							
TZ04	Rg-A/Dressed chicken/GD/GZ631/2017 x TZ04-HA								
YRDS	Rg-A/Dressed chicken/GD/GZ631/2017 x YRD-HA^{A130S}				A130S				

GZ631 YRD PRD TZ04

Figure 1. Virus and serial passage strategy used in this project. A) Recombinant virus containing different mutations on HA cleavage site used for determine HA cleavability in various cell lines. B).Interpretation of the sources of internal genes of recombinant viruses. White letter indicated the mutations on the segment. C). Serial passage of recombinant viruses in day-14 eggs.

RESULTS

1. H7N9 HA cleavage in virus-infected cells

A

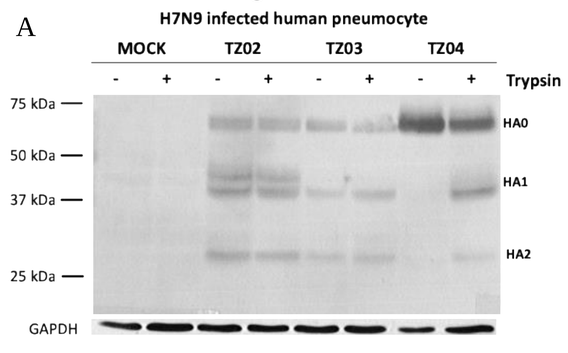

B

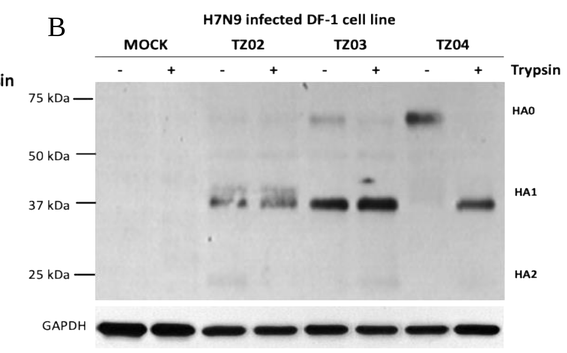

Figure 2. H7N9 HA cleavage in virus-infected cells. Human pneumocyte, or DF-1 cells were infected with TZ02 (HP H7N9) or with the mutant TZ03 (cleavage site mutated HP H7N9) or TZ04 (LP H7N9) at an MOI of 2 for 15 h in medium containing 0.2% BSA. For trypsin-treated samples, the infected cells were incubated with trypsin (1 μg/ml) for 15 min at 37° C. The cell lysate is harvest by RIPA buffer following with centrifugation at 13200 x rpm for 30 minutes to collect supernatants. The HA was visualized by Western blotting using polyclonal antibody of A/Neth/219/03.

2. Glycan array analysis of binding specificities of China H7N9 virus

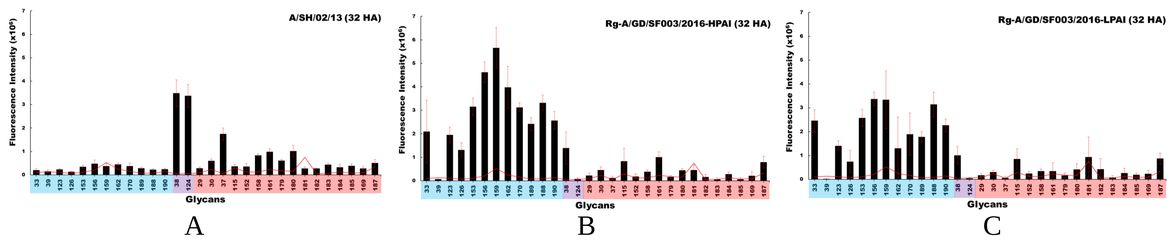

Figure 5: Glycan array analysis of binding specificities of China H7N9 virus. Recombinant A/GD/SF003/2016-HPAI (A) and A/GD/SF003/2016-LPAI virus (B) compared to the A/Shanghai/2/2013 (C) also infected a human. Colored bars highlight glycans that contain α2-3 SA (blue) α2-6/α2-3 mixed SA (purple) and α2-6 SA (red). The average binding of virus and standard error to each glycan calculated from six independent replicates on the array.

3. Growth kinetics of the recombinant parental viruses in MDCK cells and eggs

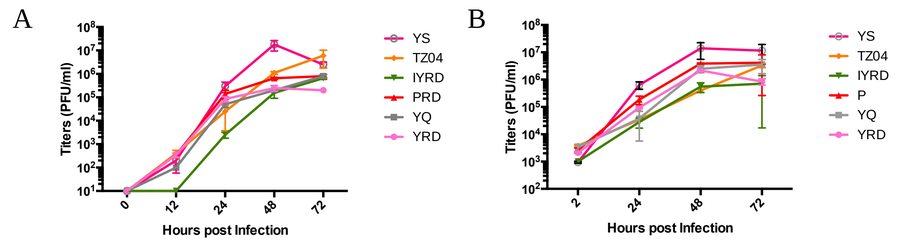

Figure 6: Growth kinetics of parental recombinant influenza viruses. (A) MDCK cells were infected with the indicated virus at an m.o.i. of 0.01. Aliquots were removed from the supernatant at 0, 12, 24, 48 and 72 h p.i. and (B) 14-day eggs were infected with indicated virus at an 10^5 PFU/egg and allantoic fluid were harvested at 2,24, 48 and 72 h p.i. Experiments were carried out induplicate and are displayed as means with standard error.

4. Distribution of vSNVs along the HA genome

Figure 7: Distribution of vSNVs along the HA gene**.** A viral Single Nucleotide Variants (vSNVs) is a position with a significant variant that has been identified in at least 1% of the samples in a group. X-axis: nucleotide position along the HA segment; Y-axis: Total frequencies of vSNV on each site were analyzed by CLC Genomics Workbench.

CONCLUSION

1. Different amino acid on the P6 position on the HA cleavage site showed discrepant cleavage abilities in various cell lines in absences of trypsin.
2. Compared with human isolated H7N9 virus in 2013, which recognize dual α2-3 and α2-6-linked glycan receptor, HPAIV H7N9 virus in 2016 showed a glycan binding profile preference on α2-3 SA and the insertion do not change glycan binding profile.
3. The G505A mutation occurred in each virus since E5 and be maintained until E10. It implicates all virus are under a similar selection condition. The insertion near the cleavage site have not been observed.

REFERENCE

1. Su W, Cheng KL, Chu DK, Zhou J, Mao X, Zhong Z, Song Y, Peiris M, Wu J, Yen HL. Genetic analysis of H7N9 highly pathogenic avian influenza virus in Guangdong, China, 2016–2017. Journal of Infection. 2018 Jan 1;76(1):93-6.

2. Quan C, Shi W, Yang Y, Yang Y, Liu X, Xu W, Li H, Li J, Wang Q, Tong Z, Wong G. New threats from H7N9 influenza virus: spread and evolution of high-and low-pathogenicity variants with high genomic diversity in wave five. Journal of virology. 2018 Jun 1;92(11):e00301-18.